

Structural and Electrical Characteristics of Ba(Fe_{0.5}Nb_{0.5})O₃-SrTiO₃ Ceramic System

Narendra Kumar Singh^{1*}, Pritam Kumar¹, Ajay Kumar Sharma¹, Ram Naresh Prasad Choudhary²

¹University Department of Physics, V. K. S. University, Bihar, India; ²Physics Department, ITER, SOA University, Bhubnesher (Orisa), India.

Email: *singh_nk_phy27@yahoo.com

Received August 27th, 2011; revised October 8th, 2011; accepted October 19th, 2011.

ABSTRACT

A complex structure of barium iron niobate, Ba(Fe_{0.5}Nb_{0.5})O₃ (BFN) and strontium titanate SrTiO₃ (ST) was fabricated by a solid-state reaction method. The phase formation of Ba(Fe_{0.5}Nb_{0.5})O₃-SrTiO₃ was checked using X-ray diffraction (XRD) technique. The X-ray structural analysis of BFN and BFN-ST ceramics, showed the formation of single-phase compound in the monoclinic system, which is a distorted structure of an ideal cubic perovskite. Careful examination of microstructures of the individual compounds of the system was done by the scanning electron micrograph (SEM), and confirms the polycrystalline nature of the systems. Detailed studies of dielectric and electrical impedance properties of the systems in a wide range of frequency (100 Hz - 5 MHz) and different temperatures (30 °C - 285 °C) showed that these properties are strongly dependent on temperature and frequency.

Keywords: Dielectrics, Perovskite Oxides, X-Ray Diffraction, Scanning Electron Micrograph

1. Introduction

Complex perovskite with general formula ABO₃ (A = mono-divalent, B = trid to hexavalent) are widely used for detectors, sensors, actuators, multi-layer ceramic capacitor (MLCC), computer memories, pyroelectric detectors, wireless communication systems, microelectronics, global positioning systems and other electronic devices. Ferroelectric perovskites have been the subject of extensive studies due to their promising electrical characteristic which has a potential usefulness in fundamental research and technological applications. Investigation of the electrical properties of these materials is desirable to predict their suitability for electronic applications. Various relaxation processes seem to coexist in complex perovskite ceramics, which contain a number of different energy barriers due to point defects appearing during their fabrication. Therefore, the departure of the response from an ideal Debye model in ceramic samples, resulting from the interaction between dipoles, cannot be disregarded. A method of predicting the relaxation behavior of a perovskite is through electric modulus theory [1].

The dielectric constant of a material (dielectric) changes due to the change of polarization by an applied electric field. This change in polarization is time dependent. Because of the resistance (resistivity) to the motion of the

atoms in the dielectric, there is always a delay between changes in the field and changes in the polarization, which gives the dissipation factor tanδ and is proportional to the energy absorbed per cycle by the dielectric from the field [2].

Alternating current (AC) impedance spectroscopy is an appropriate method to study 1) the properties of the intragranular and interfacial regions and their interrelations, 2) their temperature and frequency dependent phenomena in order to separate the individual contributions from the total impedance and 3) their interfaces with electronically conducting electrodes [3-6]. AC impedance spectroscopy allows measurement of the capacitance (C) and tangent loss (tanδ) over a frequency range at various temperatures. From the measured capacitance and tangent loss, four complex dielectric functions can be computed: impedance (Z*), permittivity (ε*), electric modulus (M*) and admittance (Y*). Studies of electrical data in the different functions and forms allow different features of the materials to be recognized.

Materials having a diffuse phase transition have attracted the most attention due to their broad maximum in the temperature dependence of their dielectric constant. The high value of the dielectric constant over a very wide temperature interval is due to disorder in the distribution

of B-site ions in the perovskite unit cell. This may lead to composition fluctuations and, as a consequence, to different local Curie temperatures in the different regions of the ceramic [7].

Recently, high dielectric permittivity (ϵ') has been reported for ternary perovskite BaFe_{0.5}Nb_{0.5}O₃ (BFN) of certain compositions. Many researchers have studied BFN, including Saha and Sinha [8], Intatha *et al.* [9], Fang *et al.* [10], Raevski *et al.* [11] Nedelcu *et al.* [12], Tezuka *et al.* [13], Yokosuka *et al.* [14] and Rama *et al.* [15]. They have reported that the BFN-based electroceramics exhibit a relaxor behavior by showing very attractive dielectric and electric properties over a wide range of temperatures. However, there still exist considerable debates concerning the physical mechanisms governing their electrical behavior [9]. In the present work, Ba(Fe_{0.5}Nb_{0.5})O₃ (BFN) and strontium titanate SrTiO₃ (ST) was fabricated by a solid-state reaction method. The dielectric characteristics of BFN(a), BFN-ST5(b) and BFN-ST10(c) ceramics are evaluated in broad temperature and frequency ranges.

2. Experimental Procedures

Complex perovskite oxides (1-x)Ba(Fe_{0.5}Nb_{0.5})O₃-xSrTiO₃, (where x = 0, 0.05 and 0.10; hereafter abbreviation as BFN(a), BFN-ST5(b) and BFN-ST10(c) respectively) were prepared by a solid-state reaction technique. High-purity ($\geq 99.9\%$) ingredients: BaCO₃, SrCO₃, TiO₂, Nb₂O₅ and Fe₂O₃ (all from M/s Merck specialities private limited), were used for the preparation of BFN(a), BFN-ST5(b) and BFN-ST10(c) ceramics. These chemicals were taken in stoichiometric ratio, and mixed in the presence of acetone for 5 h. The finely mixed powder of BFN(a), BFN-ST5(b) and BFN-ST10(c) were calcined at 1200°C for 8 h. The calcined powder of above mentioned ceramics were reground and used to make pellet of diameter ~10 mm and thickness 1 - 2 mm using polyvinyl alcohol as binder. The pellets were sintered at 1250°C for 5 h and then brought to room temperature under controlled cooling. The formation and quality of the compounds were checked with X-ray diffraction (XRD) technique. The frequency dependence of the capacitance and conductance is measured using an LCR meter in the temperature range from 30°C to 285°C and in the frequency range from 100 Hz to 5 MHz. The ac electrical conductivity $\sigma_{ac} = \omega\epsilon_0\epsilon''$ were obtained from the temperature dependence of the real (ϵ') and imaginary (ϵ'') components of the complex dielectric constant $\epsilon^* = (\epsilon' - j\epsilon'')$. The X-ray powder diffraction pattern of the sample is taken at room temperature using a X-ray powder diffractometer (Rigaku Miniflex, Japan) using CuK α radiation ($\lambda = 1.5418 \text{ \AA}$) in a wide range of Bragg angles 2θ ($20^\circ \leq 2\theta \leq 80^\circ$) with scanning rate $2^\circ/\text{min}$. The mi-

crographs are recorded using scanning electron microscopy JEOL-JSM-5800 to study the surface morphology/microstructure of the sintered pellets.

3. Results and Discussion

The room temperature X-ray diffraction (XRD) patterns of BFN(a), BFN-ST5(b) and BFN-ST10(c) ceramics is compared in **Figure 1**. The nature of XRD patterns appears to confirm the formation of single-phase with monoclinic crystal structure of the compounds. All the reflection peaks of the XRD pattern of the samples were indexed, and the lattice parameters were determined in the monoclinic crystal systems using a computer program "POWDMULT" [16].

On the basis of best agreement between the observed (obs.) and the calculated (cal.) d-spacing (*i.e.* $\sum \Delta d = d_{obs} - d_{cal} = \text{minimum}$), all the compounds were found to be in monoclinic crystal system. The room temperature SEM (scanning electron microscope) micrographs of sintered pellets of BFN(a), BFN-ST5(b) and BFN-ST10(c), ceramics are compared in **Figure 2**. The nature of the micrographs exhibits the polycrystalline texture of the material having highly distinctive and compact rectangular/cubical grain distributions. Careful examination (scanning) of the complete surface of the sample exhibits that the grains are homogeneously distributed through out the surface of the sample. The average grain size of BFN(a), BFN-ST5(b) and BFN-ST10(c), was around ~ 2 - 3 μm .

The logarithmic angular frequency dependence of the dielectric constant (ϵ') of BFN(a), BFN-ST5(b) and BFN-ST10(c), ceramics at 30°C and 130°C are plotted in **Figure 3**. At 30°C, the dielectric constant (ϵ') has a value of 367 for BFN(a), 7125 for BFN-ST5(b) and 23153 for

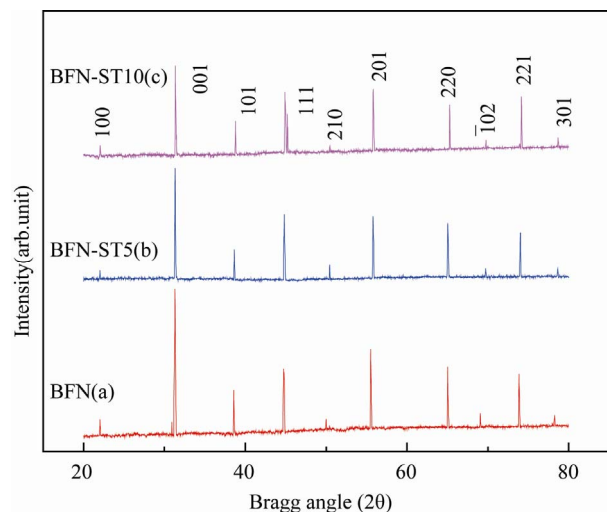
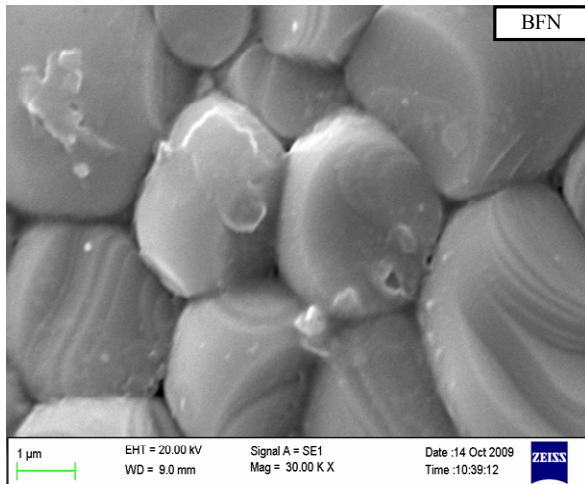
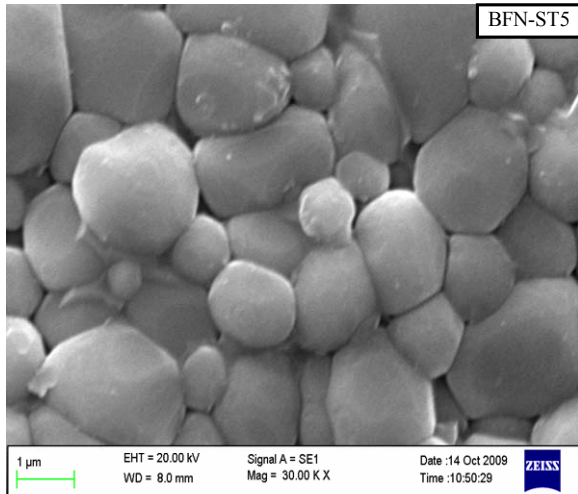


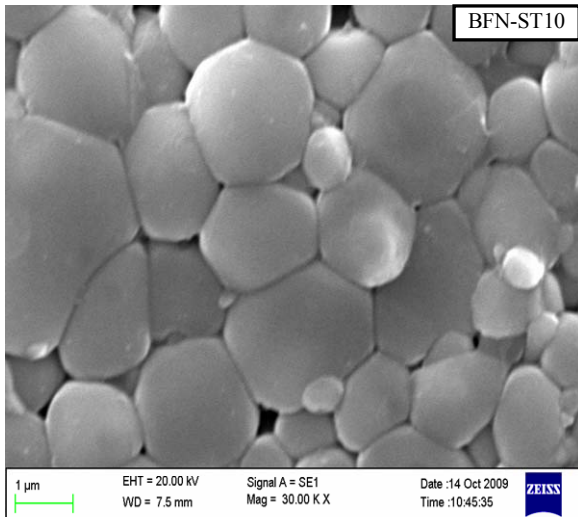
Figure 1. X-ray diffraction patterns of BFN(a), BFN-ST5(b) and BFN-ST10(c), ceramics, at room temperature.



(a)



(b)



(c)

Figure 2. SEM micrographs of BFN(a), BFN-ST5(b) and BFN-ST10(c) ceramics at room temperature at 1 μm magnification.

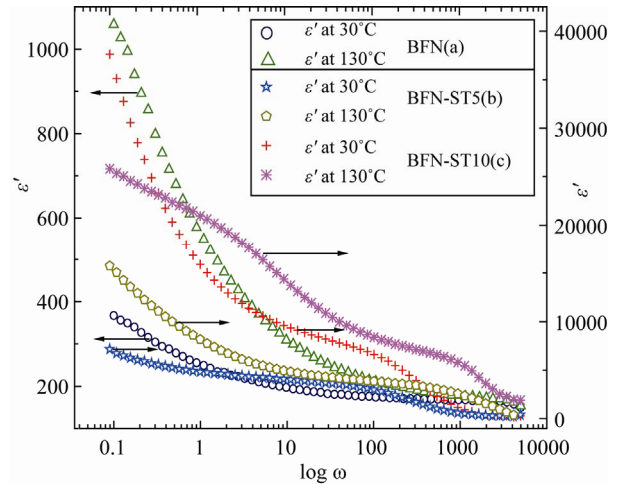


Figure 3. Frequency dependence of dielectric constant (ϵ') of BFN(a), BFN-ST5(b) and BFN-ST10(c) ceramics, at 30°C and 130°C.

BFN-ST10(c) at 100 Hz, and gradually decreases as frequency increases. But at 130°C, the value of ϵ' in the low frequency region (below 1 kHz), increases significantly for BFN(a) and BFN-ST5(b) ceramics.

This behavior is very much consistent with that of common ferroelectrics. The higher values of ϵ' at lower frequencies are due to the presence of all different types of polarizations (*i.e.*, dipolar, atomic, ionic, electronic contribution) in the material. At high frequencies, however, some of the above-mentioned polarizations may have less contribution in ϵ' . This behavior is also found in other compounds studied by us [17-22].

The high value of ϵ' in the low frequency region has been explained using Maxwell-Wagner (MW) polarization effect. Thus high values of permittivity are not usually intrinsic, but rather associated with heterogeneous conduction in the grain and grain boundary of the compounds. That is due to the grains of the sample are separated by more insulating intergrain barriers, as shown in a boundary layer capacitor [23].

The logarithmic angular frequency dependence of the loss tangent ($\tan\delta$) of above mentioned ceramics at 30°C and 130°C are plotted in inset of **Figure 4**. It is observed that $(\tan\delta)_{\max}$ maximum increases as temperature increases from 30 to 130°C, indicating that the concentration of conduction electrons increases as temperature due to thermal activation [24].

Temperature dependence of dielectric constant (ϵ') and tangent loss ($\tan\delta$) of BFN(a), BFN-ST5(b) and BFN-ST10(c), ceramics is shown in **Figure 5** and **Figure 6** respectively at selected frequencies (1 and 20 kHz), respectively. The dielectric constant (ϵ') is found to increase with rise in temperature at selected frequency for BFN(a) ceramics. One possibility for this behavior is that

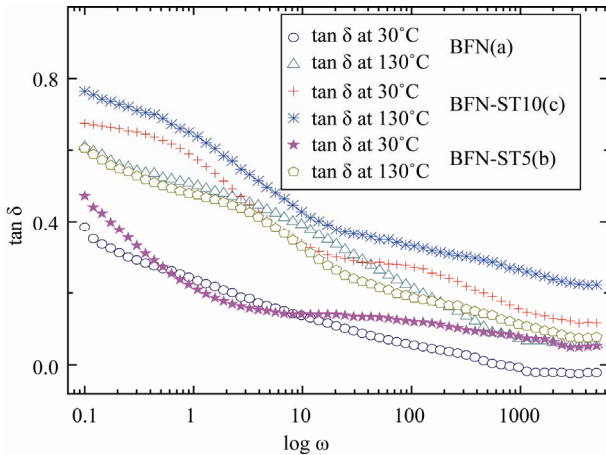


Figure 4. Variation of $\tan\delta$ with frequency of BFN(a), BFN-ST5(b) and BFN-ST10(c) ceramics, at 30°C and 130°C.

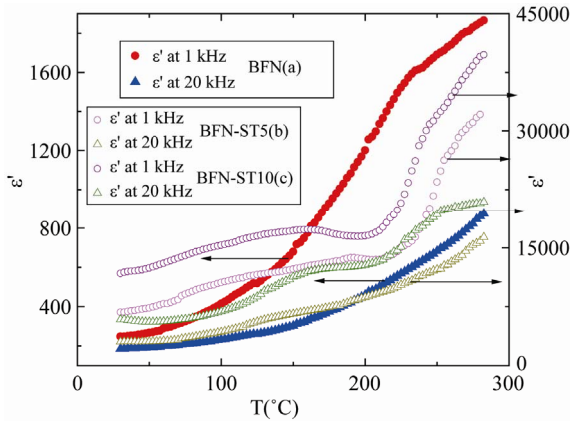


Figure 5. Variation of dielectric constant (ϵ') with temperature of BFN(a), BFN-ST5(b) and BFN-ST10(c) ceramics at 1 kHz and 20 kHz.

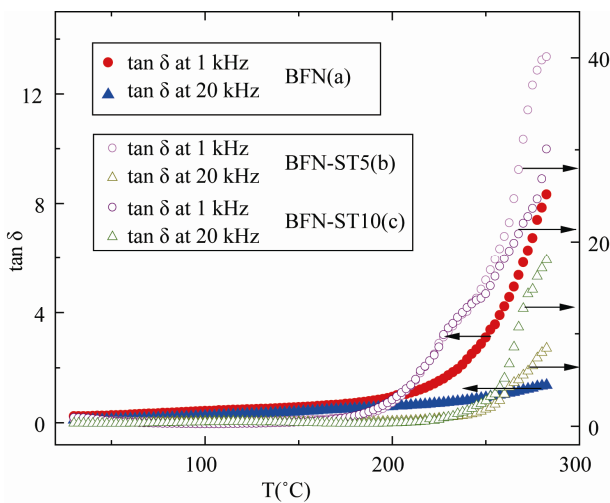


Figure 6. Variation of tangent loss ($\tan\delta$) with temperature for BFN(a), BFN-ST5(b) and BFN-ST10(c) ceramics at 1 kHz and 20 kHz.

it is due to the increased conductivity in the samples caused by the presence of Fe²⁺ in sintered BFN (a) ceramics, as suggested by Ananta and Thomas [25]. The concentration of Fe²⁺ ions is known to be very sensitive to temperature, and it increases as temperature increases [26]. It is known that the co-existence of Fe²⁺ and Fe³⁺ ions on equivalent crystallographic sites can give rise to an electron-hopping conduction mechanism. But for BFN-ST5(b) and BFN-ST10(c) ceramics, the dielectric constant increased with increasing temperature and become broad curve from 180°C onward. In addition, the dielectric constant was found to decrease with increasing frequency. This behavior may be due to fact that the dipoles are able to follow the applied voltage at low frequency, but they not follow to the field at higher frequency.

From **Figure 6**, it is clear that in the low temperature region, $\tan\delta$ is almost constant up to a certain temperature and then increases faster up to a highest temperature (~282.5°C) in BFN(a), BFN-ST5(b) and BFN-ST10(c), ceramics.

The logarithmic angular frequency dependence of Z' and Z'' of BFN(a), BFN-ST5(b) and BFN-ST10(c) ceramics, at several temperatures between 120°C and 270°C is plotted in **Figure 7**. At lower temperature, Z' (BFN (a)), Z' (BFN-ST5(b)) and Z' (BFN-ST10 (c)) decreases monotonically with increasing frequency up to certain frequency and then becomes frequency independent. At higher temperatures, Z' (BFN (a)), Z' (BFN-ST5 (b)) and Z' (BFN-ST10 (c)) is almost constant and for even higher frequencies decreases sharply.

The higher values of Z' (BFN (a)), Z' (BFN-ST5 (b)) and Z' (BFN-ST10 (c)) at low frequencies and low temperatures means the polarization is larger. The temperatures where this change occurs vary in the material with frequencies. This also means that the resistive grain boundaries become conductive at these temperatures. This also shows that the grain boundaries are not relaxing even at very high frequencies even at higher temperatures.

At lower temperatures Z'' (BFN (a)), Z'' (BFN-ST5 (b)) and Z'' (BFN-ST10 (c)) decreases monotonically suggesting that the relaxation is absent. This means that relaxation species are immobile defects and the orientation effects may be associated. As the temperature increases, the peak of Z'' (BFN-ST5 (b)) and Z'' (BFN-ST10 (c)) starts appearing. The peak shifts towards higher frequency with increasing temperature showing that the resistance of the bulk material is decreasing. Also the magnitude of Z'' (BFN-ST5 (b)) and Z'' (BFN-ST10 (c)) decreases with increasing frequencies. This would imply that relaxation is temperature dependent, and there is apparently not a single relaxation time. There by relaxa-

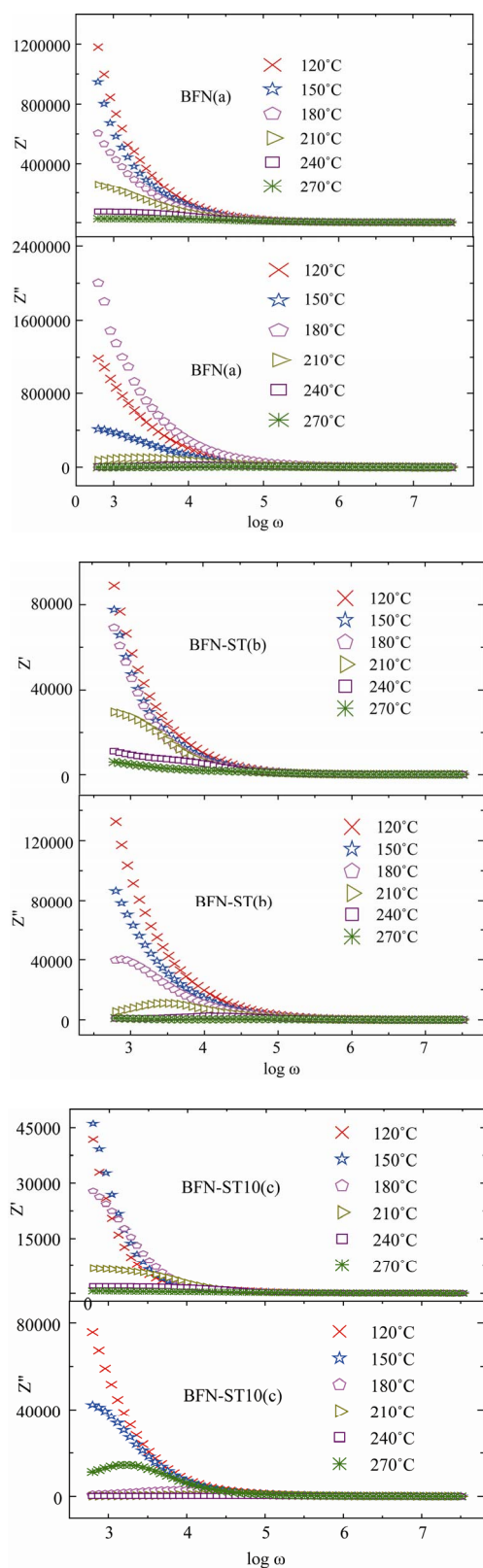


Figure 7. Variation of Z' and Z'' with frequency of BFN(a), BFN-ST5(b) and BFN-ST10(c) ceramics at various temperatures.

tion processes involved with their own discrete relaxation time depending on the temperature. Also it is evident that with increasing temperature, there is a broadening of the peaks and at higher temperatures, the curves appear almost flat.

Complex impedance spectrum Z'' vs. Z' (called as Cole-Cole plot) of BFN(a), BFN-ST5(b) and BFN-ST10(c) ceramics, at 220°C is shown in **Figure 8**. Only one semicircular arc is observed in the Cole-Cole plot confirms that the polarization mechanism in BFN(a), BFN-ST5(b) and BFN-ST10(c) ceramics. This electrical behavior can be represented in terms of an equivalent circuit (**Figure 8** BFN (a) inset). The semicircle has their center located away from the real axis, indicating the presence of relaxation species, and non-Deby type of relaxation process occurs in the materials. The appearance of single semicircle in the impedance pattern at 220°C suggests that the electrical process occurring in the material has a single relaxation process possibly due to the contribution for bulk material only.

Figure 9 shows the ac conductivity of the BFN(a), BFN-ST5(b) and BFN-ST10(c) ceramics, as a function of frequency at different temperatures. The ac conductivity of the system depends on the dielectric properties and sample capacitance of the material. The two plateaus separated by frequency region are observed in BFN (a) ceramics. The low-frequency plateau represents the total conductivity whereas the high-frequency plateau represents the contribution of grains to the total conductivity. The presence of both the high and low frequency plateaus in conductivity spectra suggests that the two processes are contributing to the bulk conduction behavior. One of these processes relaxes in the higher frequency region and contribution of the other process appears as a plateau in the higher frequency region [27]. The conductivity shows dispersion which shifts to higher frequency side with the increase of temperature. The strong frequency dependent conductivity has been found above (10 kHz) for BFN-ST5(b) and BFN-ST10(c) with the frequency independent conductivity below 10 kHz which is a typical feature of perovskite at elevated temperature (>180°C).

4. Conclusions

In this work, we reported structural, dielectric and impedance properties of barium iron niobate, Ba(Fe_{0.5}Nb_{0.5})O₃ (BFN) and strontium titanate SrTiO₃ (ST) prepared by a high-temperature solid-state reaction method. Preliminary structural analysis suggests that formation of single-phase compound in the monoclinic system. Detailed studies of electrical (dielectric, impedance and conductivity) properties exhibited a strong frequency dependent dielectric dispersion of the compound.

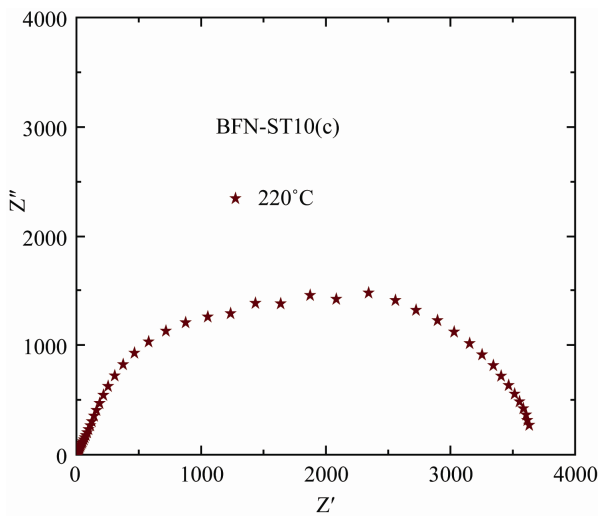
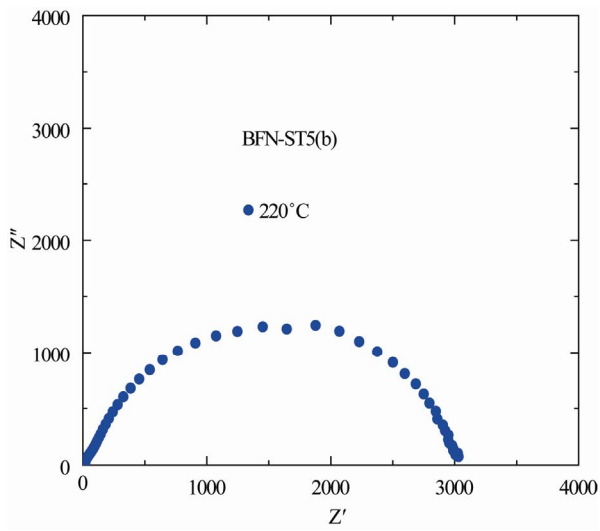
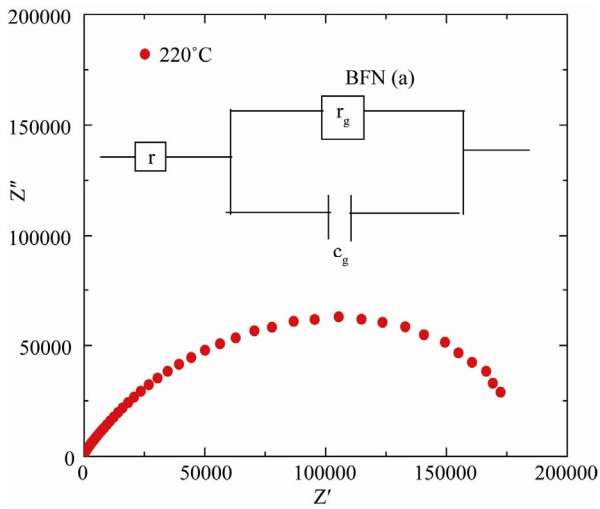


Figure 8. Complex plane impedance plot of BFN(a), BFN-ST10(b) and BFN-ST5(c) at 220°C and equivalent circuit (inset of Figure 8 (BFN (a))).

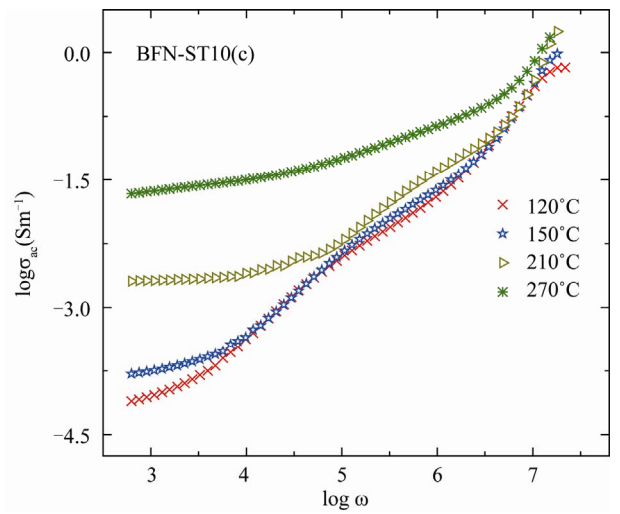
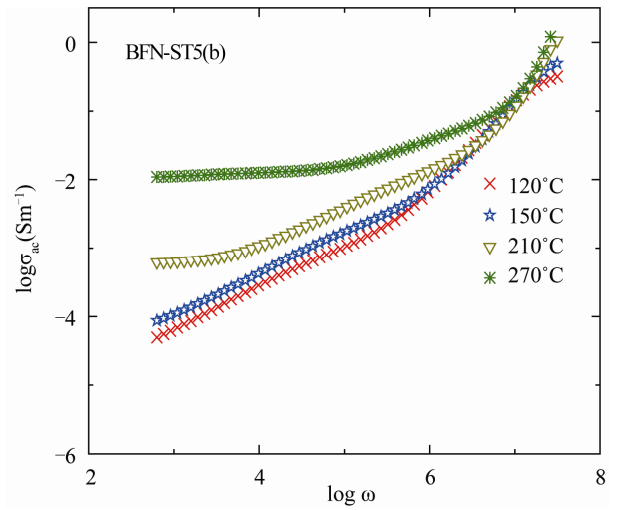
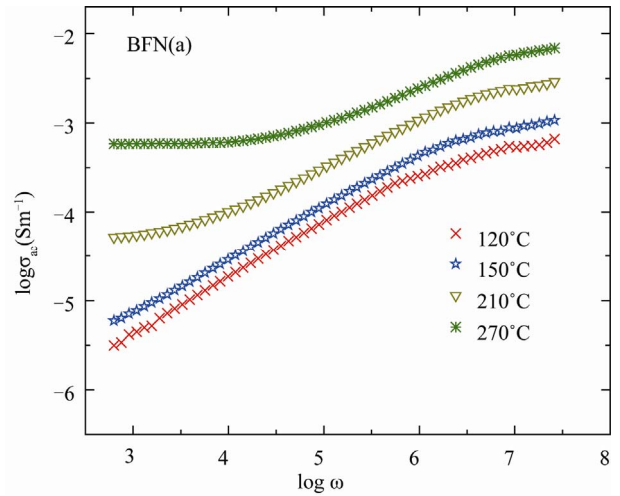


Figure 9. Variation of σ_{ac} with angular frequency for BFN(a), BFN-ST5(b) and BFN-ST10(c) ceramics, at various temperatures.

The microstructure of the ceramics was examined by the scanning electron microscopy (SEM), and shows the polycrystalline nature of the samples with different grain sizes.

5. Acknowledgements

The authors are grateful to DRDO, for providing financial assistance for this Research work.

REFERENCES

- [1] V. Prakash, A. Datta, S. N. Choudhary and T. P. Sinha, "Dielectric Relation in Perovskite Ba(Zn_{1/2}W_{1/2})O₃," *Materials Science and Engineering B*, Vol. 142, 2007, pp. 98-105. [doi:10.1016/j.mseb.2007.07.007](https://doi.org/10.1016/j.mseb.2007.07.007)
- [2] L. Agrawal, B. P. Singh and T. P. Sinha, "Dielectric Relaxation in Complex Perovskite Oxide In(Ni_{1/2}Zr_{1/2})O₃," *Materials Research Bulletin*, Vol. 44, 2009, pp. 1858-1862. [doi:10.1016/j.materresbull.2009.05.014](https://doi.org/10.1016/j.materresbull.2009.05.014)
- [3] J. R. Macdonald, "Impedance Spectroscopy Emphasizing Solid Materials and Systems," John Wiley and Sons, Inc., New York, 1987.
- [4] D. C. Sinclair and A. R. West, "Impedance and Modulus Spectroscopy of Semiconducting BaTiO₃ Showing Positive Temperature Coefficient of Resistance," *Journal of Applied Physics*, Vol. 66, 1989, p. 3850. [doi:10.1063/1.344049](https://doi.org/10.1063/1.344049)
- [5] A. K. Jonscher, "A New Understanding of the Dielectric Relaxation of Solids," *Physica Status Solidi A*, Vol. 32, 1975, p. 665. [doi:10.1002/pssa.2210320241](https://doi.org/10.1002/pssa.2210320241)
- [6] F. Roulland, R. Terras, G. Allainmat, M. Pollet and S. Marinel, "Lowering of BaB'_{1/3}B''_{2/3}O₃ Complex Perovskite Sintering Temperature by Lithium Salt Additions," *Journal of the European Ceramic Society*, Vol. 24, 2004, 1019. [doi:10.1016/S0955-2219\(03\)00553-3](https://doi.org/10.1016/S0955-2219(03)00553-3)
- [7] S. Saha and T. P. Sinha, "Law-Temperature Scaling Behavior of Ba(Fe_{0.5}Nb_{0.5})O₃," *Physical Review B*, Vol. 65, 2002, pp. 134103-134106. [doi:10.1103/PhysRevB.65.134103](https://doi.org/10.1103/PhysRevB.65.134103)
- [8] S. Saha and T. P. Sinha, "Structural and Dielectric Studies of Ba(Fe_{0.5}Nb_{0.5})O₃," *Journal of Physics: Condensed Matter*, Vol. 14, 2002, p. 249. [doi:10.1088/0953-8984/14/2/311](https://doi.org/10.1088/0953-8984/14/2/311)
- [9] U. Intatha, S. Eitssayeam, J. Wang and T. Tunkasiri, "Impedance Study of Giant Dielectric Permittivity in BaFe_{0.5}Nb_{0.5}O₃ Perovskite Ceramic," *Current Applied Physics*, Vol. 10, 2010, pp. 21-25. [doi:10.1016/j.cap.2009.04.006](https://doi.org/10.1016/j.cap.2009.04.006)
- [10] B. Fang, Z. Cheng, R. Sun and C. Ding, "Photonic & Sonic Band-Gap and Metamaterial Bibliography," *Journal of Alloys and Compounds*, Vol. 471, 2009, pp. 539-543. [doi:10.1016/j.jallcom.2008.04.056](https://doi.org/10.1016/j.jallcom.2008.04.056)
- [11] I. P. Raevski, S. A. Prosendeev, A. S. Bogatin, M. A. Malitskaya and L. Jastrabik, "High Dielectric Permittivity in AFe_{1/2}B_{1/2}O₃ Nonferroelectric Perovskite Ceramics (A = Ba, Sr, Ca; B = Nb, Ta, Sb)," *Journal of Applied Physics*, Vol. 93, 2003, p. 4130. [doi:10.1063/1.1558205](https://doi.org/10.1063/1.1558205)
- [12] L. Nedelcu, M. I. Toacsan, M. G. Banciu and A. Ioachim, *Journal of Alloys Compounds*, Vol. 509, 2011, pp. 477-481. [doi:10.1016/j.jallcom.2010.09.069](https://doi.org/10.1016/j.jallcom.2010.09.069)
- [13] K. Tezuka, K. Henimi, Y. Hinatsu, N. M. Masaki, *Journal of Solid State Chemistry*, Vol. 154, 2000, p. 591. [doi:10.1006/jssc.2000.8900](https://doi.org/10.1006/jssc.2000.8900)
- [14] M. Yokosuka, "Dielectric Dispersion of the Complex Perovskite Oxide Ba(Fe_{1/2}Nb_{1/2})O₃ at Low Frequencies," *Journal of Applied Physics*, Vol. 34, 1995, p. 5338. [doi:10.1143/JJAP.34.5338](https://doi.org/10.1143/JJAP.34.5338)
- [15] N. Rama, J. B. Philipp, M. Opel, K. Chandrasekaran, V. Sankaranarayanan, R. Gross and M. S. R. Rao, "Study of Magnetic Properties of A₂B'NbO₆ (A = Ba, Sr, BaSr; and B' = Fe and Mn) Double Perovskites," *Journal of Applied Physics*, Vol. 95, 2004, p. 7528. [doi:10.1063/1.1682952](https://doi.org/10.1063/1.1682952)
- [16] E. Wul and PowdMult, "An Interactive Powder Diffraction Data Interpretation and Index Program," version 2.1, School of Physical Science, Flinders University of South Australia, Bedford Park, S.A. 5042, Australia.
- [17] N. K. Singh, P. Kumar, H. Kumar and R. Rai, "Structural and Dielectric Properties of Dy₂(Ba_{0.5}R_{0.5})₂O₇ (R = W, Mo) Ceramics," *Advanced Materials Letters*, Vol. 1, 2010, pp. 79-82. [doi:10.5185/amlett.2010.3102](https://doi.org/10.5185/amlett.2010.3102)
- [18] N. K. Singh, P. Kumar, O. P. Roy and R. Rai, "Structural, and Dielectric Properties of Eu₂(B'_{0.5}B''_{0.5})₂O₇ (B' = Ba; B'' = Mo, W) Ceramics," *Journal of Alloys and compounds*, Vol. 507, 2010, pp. 542-546. [doi:10.1016/j.jallcom.2010.08.015](https://doi.org/10.1016/j.jallcom.2010.08.015)
- [19] N. K. Singh, R. N. P. Choudhary and B. Banarji, "Dielectric and Electrical Characteristics of Nd₂(Ba_{0.5}R_{0.5})₂O₇ (R = W, Mo) Ceramics," *Physica B*, Vol. 403, 2008, p. 1673. [doi:10.1016/j.physb.2007.09.083](https://doi.org/10.1016/j.physb.2007.09.083)
- [20] P. Kumar, B. P. Singh, T. P. Sinha and N. K. Singh, "Ac conductivity and Dielectric Relaxation in Ba(Sm_{1/2}Nb_{1/2})O₃ Ceramic," *Physica B*, Vol. 406, 2011, pp. 139-143. [doi:10.1016/j.physb.2010.09.019](https://doi.org/10.1016/j.physb.2010.09.019)
- [21] N. K. Singh, P. Kumar and R. Rai, *Journal of Alloys and compounds*, Vol. 509, 2011, pp. 2957-2963. [doi:10.1016/j.jallcom.2011.01.153](https://doi.org/10.1016/j.jallcom.2011.01.153)
- [22] P. Kumar, B. P. Singh, T. P. Sinha and N. K. Singh, *Advanced Materials Letters*, Vol. 2, No. 1, 2011, pp. 76-79. [doi:10.5185/amlett.2010.11176](https://doi.org/10.5185/amlett.2010.11176)
- [23] Y. J. Li, X. M. Chen, R. Z. Hou and Y. H. Tang, "Maxwell-Wagner Characterization of Dielectric Relaxation in Ni_{0.8}Zn_{0.2}Fe₂O₄/Sr_{0.5}Ba_{0.5}Nb₂O₆ Composite," *Solid State Community*, Vol. 137, 2006, p. 120.
- [24] P. Q. Mantus, "Dielectric Response of Materials: Extension to the Debye Model," *Journal of the European Ceramic Society*, Vol. 19, 1999, p. 2079. [doi:10.1016/S0955-2219\(98\)00273-8](https://doi.org/10.1016/S0955-2219(98)00273-8)
- [25] S. Ananta and N. W. Thomas, "Relationships between Sintering Conditions, Microstructure and Dielectric Properties of Lead Iron Niobate," *Journal of the European Ceramic Society*, Vol. 9, 1999, p. 1873. [doi:10.1016/S0955-2219\(98\)00290-8](https://doi.org/10.1016/S0955-2219(98)00290-8)

- [26] K. Singh, S. A. Band and W. K. Kinge, "Effect of Sintering Temperature on Dielectric Properties of Pb(Fe_{1/2}-Nb_{1/2})O₃ Perovskite Material," *Ferroelectrics*, Vol. 306, 2004, p. 179. [doi:10.1080/00150190490460821](https://doi.org/10.1080/00150190490460821)
- [27] A. Dutta, C. Bharti and T. P. Sinha, "AC Conductivity and Dielectric Relaxation in CaMg_{1/3}Nb_{2/3}O₃," *Materials Research Bulletin*, Vol. 43, 2008, pp. 1246-1254. [doi:10.1016/j.materresbull.2007.05.023](https://doi.org/10.1016/j.materresbull.2007.05.023)